Design development of planar optical waveguide structures and diffraction gratings based on thin-film lithium niobate and titanium dioxide layers

© P.V. Volkov[1], P.A. Bushuykin[1], K.V. Sidorenko[2,¶], A.V. Zdoroveyshchev[2], G.A. Lemeshevskaya[2], D.S. Klementyev[2], I.V. Samartsev[2], A.I. Bobrov[2]

[1] Institute for Physics of Microstructures, Russian Academy of Sciences, 603950 Nizhny Novgorod, Russia
[2] Lobachevsky State University of Nizhny Novgorod, 603022 Nizhny Novgorod, Russia

¶ E-mail: sidorenko@nifti.unn.ru

Received December 24, 2025
Revised June 26, 2026 Accepted July 29, 2026

Numerical modeling of a planar strip-loaded optical waveguide based on titanium dioxide and thin-film lithium niobate has been carried out. For various values of the geometric parameters of the structure under study, and taking into account the measured optical characteristics of the TiO_2 and $LiNbO_3$ layers, the single−mode condition, the area of the fundamental transverse-electric mode, and the fraction of the optical radiation power propagating in the lithium niobate layer were obtained. The optimal values of the TiO_2 strip width and thickness, in terms of minimizing optical losses, were found to be 1.1 μm and 150 nm, respectively. An original design of highly efficient diffraction gratings for 9 coupling on a thin-film $TiO_2/LiNbO_3$ hybrid platform has been developed.

Keywords: thin-film lithium niobate, loaded waveguide, single-mode condition, refractive index, diffraction gratings.

DOI: 10.61011/SC.2026.04.64078.8928

1. Introduction

A trend in the modern world is rapid development of information technologies accompanied by a multiple increase in the volume of the processed, transmitted, and stored information. Besides, the evolution of the current electronic systems has practically reached its climax and requires the introduction of fundamentally new approaches for satisfying the always growing needs. One of such approaches is the use of the quantum photon technology for solving various problems in the area of data transmission, high performance computing, and metrology. One may distinguish among them the design of superfast quantum computers and long-range quantum distributed networks, as well as the development of sensors, visualizers, spectroscopes.

One of the most important manmade materials widely used in the field of photon technologies from the moment of discovery of its ferroelectric properties in 1949 [1] and until now is lithium niobate ($LiNbO_3$, LN). Compared to other materials, lithium niobate has some unique characteristics, such as a wide range of transparency, high electrooptic, non-linear-optic, acoustooptic and pyroelectric coefficients, as well as stable chemical and physical properties [2].

The above unique features of lithium niobate made it possible to create various photon devices on its basis. For example, due to high electrooptic coefficients of LN, high-speed modulators were developed on the basis of LN and are widely used in the current backbone fiber optic communication systems, operating using the Mach–Zehnder interferometer pattern [3].

Currently due to the development of the hetero-integration technology (XOI) [4] thin-film lithium niobate (TFLN) holds the leading position as the platform for the development of microwave photonics devices. Use of the TFLN platform allows developing waveguides directly from LN due to the application of high resolution lithography and reactive ion etching. Such waveguides have superlow optical losses ~ 2.7 dB/m [5] (compared to the losses 40−100 dB/m in waveguides obtained by diffusion of Ti [6]) and are characterized by low technological formation temperatures. Therefore, TFLN, due to a unique combination of such properties as a wide window of transparency (0.35−5 μm), high electrooptic coefficient (r33 ~ 31 pm/V) and compatibility with the complementary metal–oxide–semiconductor (CMOS)-technologies, provides for effective and linear modulation of radiation, opens the prospects for the operation in various spectral ranges, is potentially promising for serial production [7–9].

Despite the above advantages, the TFLN platform faces a serious fundamental problem — mode-field mismatch between a submicron waveguide and a standard thicker (125 μm) optic fiber. This results in lower efficiency of radiation input/output and increases the optical insertion losses. High losses from radiation input/output are a key limiting factor, which directly reduces the dynamic range and the signal-noise ratio of the entire system [10,11]. To solve this problem, the researchers consider two main approaches: end input, which consists in the direct coupling of optic fiber and the end of the photonic integrated

circuit (PIC), and vertical input using diffraction gratings.

The end input is technologically complicated for implementation on TFLN. It requires high precision polishing of the chip edges, formation of adiabatic tapers to match the modes, and precision alignment in assembly. Besides, the use of the end input limits the arrangement of the optical ports only at the crystal perimeter, reducing the layout flexibility. All these factors significantly increase the cost of assembly of the end device. Nevertheless, when the end input is used, it is possible to get a rather high efficiency factor (EF) of the coupling, for example, paper [12] demonstrates the option of the input with the losses -1.2 dB per end.

Contrary to the end input, the vertical input based on diffraction gratings [13] is devoid of the specified faults. Diffraction gratings allow placing input/output ports in any point of the chip surface, providing for 2D scalability of PIC. They have large allowances for the alignment of the fiber, which makes the assembly less expensive, and make it possible to effectively test the circuits at the wafer level, which is critical for reduction of the prime cost in serial production.

The design of the diffraction gratings is inextricably linked to the method of formation of the waveguide PIC channels. The most direct approach is the actual etching of TFLN, since it provides for the monolithic nature of the final structure. Despite this, this approach is associated with the technological complexities of deep etching of TFLN to achieve the ideal surface of the side walls (verticality and no roughness) [1,14]. Despite the complexities, paper [15] is one of the first papers, which demonstrates the successful vertical input of radiation into the TFLN-waveguide with the coupling efficiency of ~ -10 dB. The attempt to bypass the complexities of TFLN etching is the use of metal diffraction gratings. In particular, in the study [16] they used a periodical structure from golden nanorods applied onto a solid LN-waveguide for the vertical input of radiation. This method made it possible to achieve the coupling efficiency — of ~ -5 dB, and its main advantage is manufacturability, since it excludes the stage of deep etching of lithium niobate, being limited to the standard processes of metal sputtering and lithography. Note that the metal nature of the grating inevitably contributes the additional optical losses for absorption, causes heating of the structure with the increased power of radiation, and thus fundamentally limits the potential efficiency of such approach.

The alternative method of increasing the coupling efficiency is the use of a reflecting layer arranged under the waveguide. This approach enables redirecting the radiation, which would otherwise be lost in the substrate, back in the direction of the optic fiber. As it follows from papers [17–19], this principle is successfully used in the photon platforms based on silicon-on-insulator and allows achieving the coupling efficiency of ~ -3 dB. For the TFLN platform [20] the use of the metal reflectors (for example, gold) under the LN-waveguide and the metal diffraction grating makes it possible to significantly increase the coupling efficiency of the waveguide to ~ -2 dB. Note that the technological implementation of such method is associated with certain difficulties, since it requires formation of a reflecting layer at the stage of TFLN wafer preparation prior to the processes of lithography and etching of the waveguide layer, and the use of reflectors from metal limits the maximum power of radiation input into the waveguide.

Another promising approach to form both the diffraction gratings and the waveguides as such on the TFLN platform is the use of the loading layer — an additional dielectric material with high refractive index, which is applied on top of the lithium niobate film. In such hybrid structures the light mode is concentrated near the boundary between the LN and the loading layer, which allows effectively controlling the radiation propagation. Therefore, in this approach to form the pattern of PIC optic elements, it is not necessary to perform the deep etching of TFLN, but rather you can limit yourself to just etching of the loading layer. The loading layer may be, for example, silicon [21] or a more popular and technologically utilized silicon nitride Si_3N_4 [22]. The efficiency of coupling between such waveguides and the vertical input of radiation is -4 — -5 dB.

Therefore, the use of the loading layer for the formation of waveguides and diffraction gratings is a rather technologically simple and promising approach. It allows avoiding the fundamental difficulties inherent in deep etching of lithium niobate, excludes the need to create a buried metal reflecting layer with the preservation of a low value of optical losses of a passive waveguide and high coupling efficiency. Such solution significantly simplifies the PIC fabrication process and reduces its cost.

In this paper it is proposed to use titanium dioxide (TiO_2) as the loading layer. The selection of the titanium dioxide is due to its high refractive index (~ 2.5), wide transparency band, technological compatibility with the standard CMOS-processes, high coupling efficiency of radiation input using a TiO_2-diffraction grating (-4 dB [23]), potentially low optical losses of passive TiO_2-waveguides, high power characteristics of waveguides.

The quality of operation of any PIC directly depends on the parameters of its main units: the element of optical radiation input into the waveguide transmission line and the waveguide transmission line as such. The purpose of this paper is to study the effect of geometric parameters on the functioning of individual PIC elements, as well as to find their optimal values.

2. Results of mathematical modeling of planar waveguides

In order to be able to design complicated PIC units, such as diffraction gratings, directional couplers or multimode interferometers, it is necessary to perform the mathematical

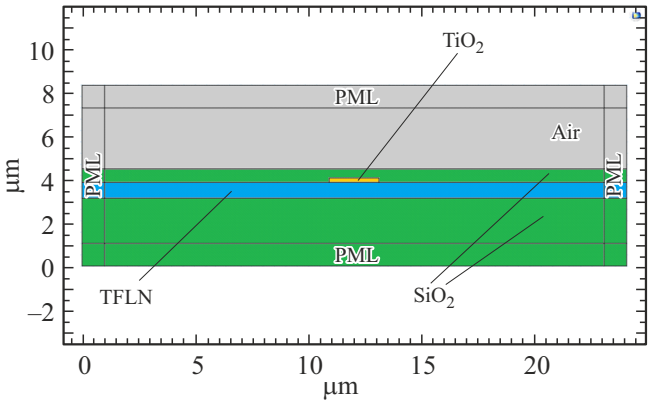


Figure 1. Computational domain of the mathematical model of the planar waveguide structure SiO_2/TFLN/TiO_2/SiO_2/Air. The perfectly matched layer is specified at the boundaries of the computational domain.

modeling of a simple waveguide structure. Therefore, first we performed the mathematical modeling of the cross section of the loaded waveguide based on a thin-film lithium niobate to optimize its geometric parameters. In our model the waveguide structure was a film of lithium niobate of x-cut section on a substrate from SiO_2 with a deposited strip of titanium dioxide. On top the structure is closed with a coating layer from SiO_2. The circuit diagram of the considered planar strip waveguide and parameters and dimensions of the computational domain are shown in Figure 1.

The mathematical modeling was performed using software suite Comsol Multiphysics with the wave optics module. Modeling consisted in the analysis of the mode composition of the cross section of the waveguide structure. To correctly describe the leaking modes, boundary conditions of scattering were used, as well as perfectly matched layers (PML) at the boundaries of the computational domain.

The thickness of the lithium niobate film was 700 nm, the thickness of the coating layer of SiO_2 — 600 nm. The refractive indices of materials were measured on real structures by the method of spectroscopic ellipsometry using an ellipsometer PhE-102 (Angstrom Advanced Inc., USA). The values of refractive indices at the wavelength of $\lambda = 1550$ nm are given in Table 1. The variable geometric parameters that we considered were width and thickness of the titanium dioxide strip deposited on the surface of the lithium niobate film. The strip width w varied from $-2\,\mu$m, for thickness h three most convenient values from the technological point of view were selected: 100, 150, and 200 nm.

The devices of waveguide photonics use only single-mode waveguides to avoid intermode dispersion and additional optical losses [24]. Therefore, the geometric parameters of cross section of the waveguide must be selected so that only the fundamental mode of radiation is maintained.

Table 1. Refractive indices of materials used in the model

Material	Value of refractive index at the wavelength $\lambda = 1550$ nm
SiO_2	1.46 ± 0.05
$LiNbO_3$ (ordinary)	2.21 ± 0.05
$LiNbO_3$ (extraordinary)	2.13 ± 0.05
TiO_2	2.50 ± 0.05

The compliance with the single mode nature condition was tested by the method proposed in paper [25]. First a quasi unidimensional laminar structure SiO_2/TFLN/SiO_2/Air without a strip TiO_2 is considered. The quasi unidimensional nature in this case means symmetry in the lateral plane. The effective index n (1D) was calculated for the main transverse-electric (TE)-mode („vertical fundamental 1D mode"). Then the effective index of the first excited TE-mode n_{eff} was calculated for the studied waveguide. For the excited mode to be propagating, it is necessary to comply with the condition $n_{\text{eff}} > n(1\text{D})$. Otherwise the excited mode will be leaking, and the waveguide will be single-mode. As a result, the following conditions of the single mode nature were obtained: for thickness of the strip TiO_2 $h = 100$ nm the width must be $w \leq 1.8\,\mu$m, for $h = 150$ nm the width must be $w \leq 1.5\,\mu$m, for $h = 200$ nm the width must be $w \leq 1.3\,\mu$m.

Other important characteristics of waveguide structures based on TFLN are the surface area of the mode and the share of the power of optical radiation accounting for the layer of lithium niobate PLN/Pwhole [26]. The losses for absorption in this spectral range are negligibly low. The losses for scattering are also lower since the main part of the mode is submerged into lithium niobate and does not contact with the irregularities on the side faces of the strip TiO_2. Therefore, the main mechanism of losses in such waveguides is radiation loss. These losses increase as the bending radius of the waveguide decreases, and as the mode surface area increases. Therefore, for this acceptable level of losses we can make the PIC units more compact due to the decrease in the waveguide bending radius, if we are able to confine the optical mode more.

On the other side, the elements of phase shift, the operation principle of which in the structures on the TFLN platform is based on the electrooptic effect, may also be made more compact due to the increase in the overlap integral between the control electric field and the electric field of the propagating optical mode. Since the material TiO_2 has no electrooptical effect, the overlap integral will depend on the share of the power of radiation propagating inside lithium niobate.

Figure 2 presents the dependences of the surface area of the fundamental optical TE-mode and the share of the power of radiation in lithium niobate on geometric parameters of cross section of the waveguide. The surface

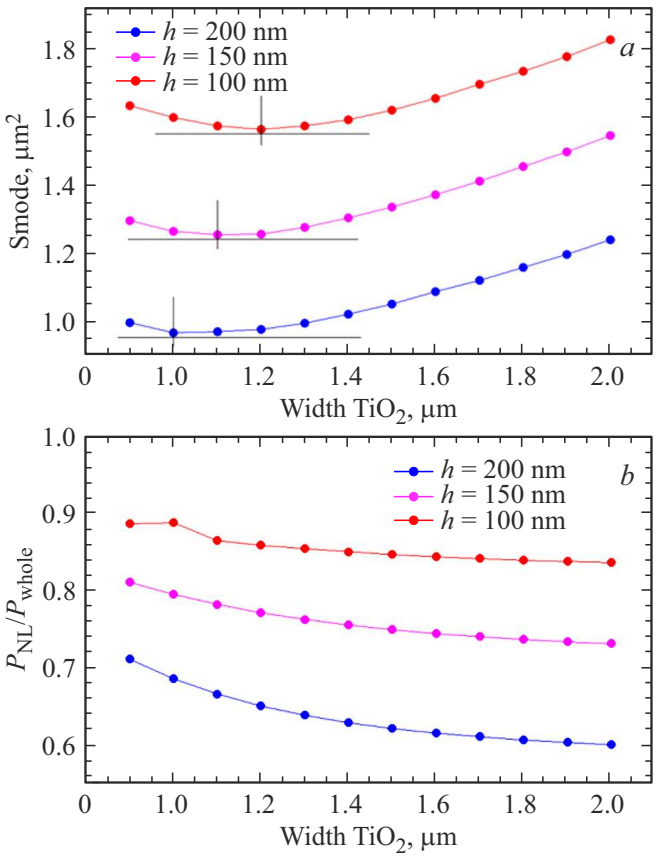


Figure 2. Dependences of the surface area of the fundamental optical TE-mode (a) and the share of the radiation power in lithium niobate for the fundamental optical TE-mode (b) on geometric parameters of cross section of the waveguide.

area of the mode in this case means that part of the cross section of the waveguide, inside which the density of the power of the propagating optical radiation is $1/e$ from the maximum power and higher.

From the dependences shown in Figure 2, a you can see that as the thickness of the strip TiO_2 increases, the surface area of the optical mode decreases. Besides, each of the dependences of the mode surface area on the strip width has a specific minimum near the value of $w = 1.1\,\mu$m. In its turn from the data given in Figure 2, b you can see that as the thickness or width of the strip TiO_2 increases, the share of the power of optical radiation in the layer of lithium niobate monotonically decreases. These dependences may be explained by the fact that titanium oxide has a refractive index, which is significantly higher compared to lithium niobate (2.5 vs. 2.13 for the TE-mode). Therefore, the strip TiO_2 as its transverse geometric dimensions increase, takes the larger part of the optical power for itself, and the radiation mode is localized within the strip boundaries.

From the practical point of view the optimal value of the TiO_2 strip width is the value of $w = 1.1\,\mu$m, since the surface area of the mode for any thickness of the strip is located near the minimum (Figure 2, a), and the share of the power of radiation in lithium niobate is close to the maximum value (Figure 2, b). To select the optimal value for the thickness of the strip TiO_2, the following assumption was considered: as the thickness of the strip increased by 50 nm (from 100 to 150 nm) the value P_{LN}/P_{whole} decreases slightly ($\sim 10\,\%$), whereas the surface area of the mode decreases by $\sim 25\,\%$, which significantly decreases the losses for radiation at the waveguide bends. Besides, the heavy thickness of the strip ($h = 200$ nm) causes appearance of some negative features, namely, the roughness of the TiO_2 strip walls increases, and the material homogeneity in the surface area decreases. These features that deteriorate the strip characteristics are hard to remove technologically. Based on the above, the optimal value of the strip thickness was the value of $h = 150$ nm.

3. Mathematical modeling of diffraction gratings

The problem of the effective bond between the single mode optic fiber (OF) and PIC is one of the key problems for the development of end devices. As it was mentioned above, one of frequently used methods is the use of diffraction gratings (DG) due to their significantly better manufacturability compared to the end solutions. When the waveguide is formed by etching of the layer $LiNbO_3$, DGs are also usually formed directly in $LiNbO_3$ [27]. Formation of such gratings is a technologically complicated procedure in virtue of the problems with the etching of $LiNbO_3$, which were noted above. Accordingly, when the loading strips are used, DGs may also be formed in the loading layer. However, this approach is limited in efficiency due to low optical thickness of the layer, and accordingly not very high efficiency of diffraction on such grating. In particular, in paper [28] the material to form the waveguide was Si_3N_4, where the DG was formed. The efficiency of such grating was $\sim 35\,\%$ (-4.7 dB), besides, it is not possible to get higher efficiency for the periodical grating on this material. Since the refractive index TiO_2 is close to the refractive index of Si_3N_4, the theoretical limit of efficiency for the DGs arranged in the layer TiO_2 is approximately at the same level.

Note that since TiO_2 was rarely used as a layer forming a waveguide in the TFLN structures, there are no papers for the development of effective DGs for such structures. Note paper [23], in which the layer TiO_2 is used in the area of formation of the surface metal DG, and the waveguide as such is formed with the help of the etching of layer $LiNbO_3$. The structure proposed in our work with the silicon DG above the layer TiO_2 has not been previously considered in the papers.

It is known that rather high efficiency of DGs in the structures with etching of $LiNbO_3$ was obtained when high contrast material was applied on the surface of $LiNbO_3$, and DGs were formed in it. For example, in paper [29]

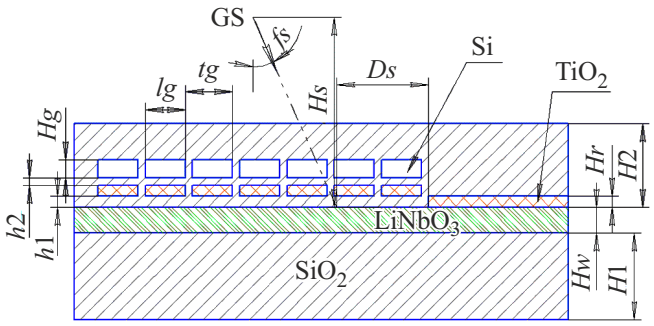


Figure 3. Double DG for the TFLN-structure. The following notations were used: $H1$ — thickness of the bottom layer SiO_2; Hw — thickness of the layer $LiNbO_3$; Hr — thickness of the layer TiO_2; $H2$ — full thickness of the structure above the layer $LiNbO_3$; $h1$ — thickness of the layer SiO_2 between $LiNbO_3$ and DG in the layer TiO_2; $h2$ — thickness of the layer SiO_2 between TiO_2 and silicon DG; Hg — thickness of the silicon DG; lg — width of the strip of the silicon DG; tg — period of the silicon DG; Ds — distance from the edge of the DG to the center of the light spot; Hs — height of the source; fs — angle of incidence of optical radiation.

the grating was made from gold, and in paper [30] — from silicon. Since in our case the waveguides were formed at the expense of the loading strips, the DG manufacture on the surface of directly $LiNbO_3$ noticeably complicates the technological process. In paper it was proposed to form a hybrid grating made of two layers. The first DG was formed in the layer TiO_2, then the protective layer SiO_2 is applied, then the Si layer is applied, where the second DG is formed. The diagram is presented in Figure 3.

The first DG in the layer TiO_2 is formed simultaneously with the loading strips, which minimizes the ability to damage the surface of $LiNbO_3$. Besides, the protective layer SiO_2 applied on top of the first DG serves as a stop layer when etching the DGs in Si and allows forming a pattern with good quality.

The condition of Bragg diffraction for DGs may be recorded as [31]

$$n_{\text{eff}} - n_1 \sin\theta_1 = \frac{\lambda}{\Lambda}, \qquad (1)$$

where n_1 — refractive index of the coating layer of DG, θ_1 — angle of incidence of radiation on DG, λ — wavelength of incident radiation, Λ — DG period, n_{eff} — effective refractive index of DG. In the first approximation the effective refractive index of the grating (n_{eff}) may be determined using the effective refractive indices of the etched grooves (n_e) and non-etched areas (n_o) [31]:

$$n_{\text{eff}} = F \cdot n_o + (1 - F) \cdot n_e. \qquad (2)$$

Therefore, the effective refractive index of the grating (n_{eff}) turns out to be dependent both on the filling factor F and on the depth of etching of the grating grooves, since the increase in the depth of etching causes a decrease in the refractive index of the grooves (n_e). It is obvious that within this approximation the change in the geometric parameters of DGs may be compensated by the change in the angle of incidence of radiation, however, the expression (1) does not allow assessing the efficiency of radiation input. For the precise analysis, the numerical methods are used, but many dependences may be understood from the common assumptions. Thus, the change in the thickness of the layer SiO_2 under the silicon DG $(h2)$ has practically no impact on diffraction, but changes the position of the diffracted wave relative to the waveguide, which changes the overlap integral and accordingly the efficiency of the radiation input. According to the modeling, the optimal thickness of this layer is in the range of 60–120 nm, and the specific value depends on the optimal angle of incidence of radiation and on the waveguide parameters. The DG thickness must also have the optimum, since small thickness will cause low efficiency of diffraction, and at heavy thickness the overlap integral between the diffracted wave and the waveguide mode will be minor. Modeling shows that the optimum is in the range of 150–300 nm and depends on other parameters of the structure. Strong mutual dependence of the parameters causes many local extrema with close results from the point of view of the radiation input/output efficiency, which complicates the search for the global extremum.

Table 2. Basic parameters of the structure

$H1$, μm	Hw, μm	$H2$, μm	Hs, μm
2	0.7	2	9

The structure was modeled in the suite ANSYS Lumerical by the FDTD method in 2D approximation. Radiation from the single mode optic fiber was approximated with Gaussian beam with the beam waist width of 10 μm, which describes very well the standard OF at wavelength of 1.55 μm.

Some parameters of the structure were fixed, and the optimization search was carried out in the others using the swarm method. The fixed parameters are given in Table 2.

The fixed parameters were selected on the basis of the following assumptions. Thickness of layer SiO_2, equal to 2 μm, is typical for silicon-on-insulator (SOI) wafers used in photonics, since it provides good insolation of the field of the waveguide mode against leaking into the substrate. The thickness of the layer $LiNbO_3$ equal to 0.7 μm is typical for the TFLN-structures and makes it possible to obtain high efficiency of the electrooptical effect in the waveguide propagation of the light. The thickness of the coating layer SiO_2 and the height of the source above the surface hardly influence the result and were selected from the assumptions of calculation convenience. The target parameter in optimization

Table 3. Optimal values of parameters for a double DG

Hr, μm	tg, μm	lg/tg	$h1$, μm	$h2$, μm	Hg, μm	fs, circ	Ds, μm
0.15	0.83	0.62	0	0.07	0.25	18.7	5

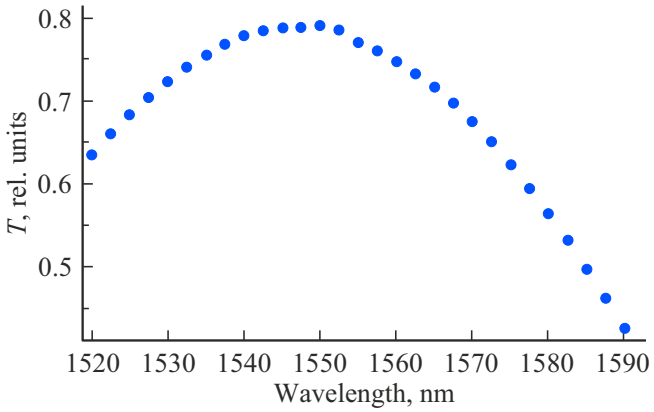


Figure 4. Spectral dependence of the input efficiency for a double DG, with optimal parameters.

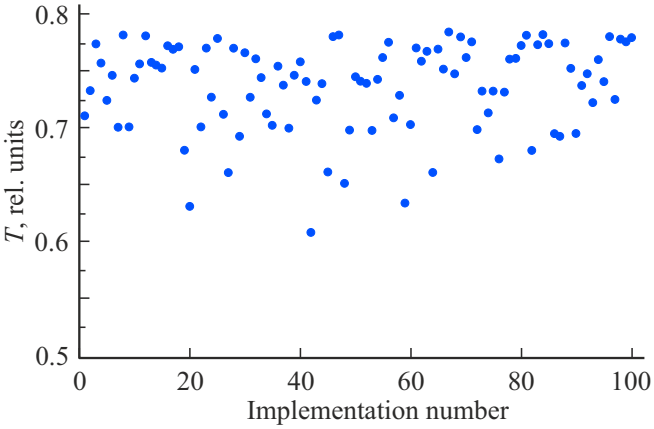


Figure 5. Spread of radiation input efficiency at random variation of DG thickness, length of DG grooves and thickness of the layer TiO_2.

was the coupling efficiency between the OF and PIC. The results of the optimization search are given in Table 3.

Here it is necessary to note that the optimal values for the thickness of the layer TiO_2 in DG and in the planar waveguide fully coincide.

Let us define the efficiency of the grating as the ratio of the power supplied to the waveguide to the power incident on the top layer of the entire structure. Figure 4 shows the spectral dependence of the efficiency of radiation input at optimal parameters of the structure.

The maximum efficiency of the input is observed near the wavelength of 1550 nm and is equal to 78.7 %, which is a very good result compared to the DGs formed directly in the layer TiO_2. The width of the working band of such DG at the level of -1 dB is 53 nm, which is more than the width C of the band of (dense wavelength division multiplexing) in DWDM wavelength grid (35 nm) and is close to the width of L of the range (60 nm).

Note that all the values of the structure parameters obtained in process of optimization are achievable technologically within the standard processes. Thicknesses of the layers are in the range of 100–300 nm, which is easily implementable by the state-of-the-art methods for thin film deposition. The DG period was 0.83 μm, which may be implemented using photolithography of not the highest resolution, for example, within the CMOS process with the technological norms of 350 nm. Note separately that the optimal value of the thickness of the layer SiO_2 under the grating in TIO_2 is 0. Therefore, in the optimal configuration the first DG is in the same technological layer with the loading strips and is made from the same material, which minimizes the number of technological operations.

The important issue is the resistance of the solution to the technological spread of parameters. To assess this impact, the final model was supplemented with a random spread of parameters. The thickness of DG and the thickness of the layer TiO_2 varied in the range of ± 10 nm from the optimal value (Table 3). And additionally the spread of the length of DG grooves was added in the range of ± 20 nm, and the length of each grating line was varied independently. 100 random configurations were modeled in the specified range of parameters spread. The obtained dependence of the radiation input efficiency was given in Figure 5. You can see that approximately for 90 % of implementations the radiation input efficiency is in the range of 70–78 %, which is the acceptable result.

Therefore, the proposed diagram of the double DG makes it possible to obtain high efficiency of the optical radiation input in PIC from the single mode OF without substantial complication of the technological process and without etching $LiNbO_3$.

4. Conclusion

Within this article, the complex mathematical modeling of the main PIC units on the TiO_2/TFLN platform was performed: the waveguide transmission line and the diffraction grating. Based on the conditions of the single mode nature, and also within the study of the geometric parameters impact on the surface area of the mode and the share of the power of the radiation localized in the lithium niobate layer, the optimal values were obtained for the width ($w = 1.1\,\mu$m) and thickness ($h = 150$ nm) of the loading strip TiO_2.

The paper proposed the design of the highly effective hybrid double-layer diffraction grating as the radiation input element in the waveguide transmission line. The

geometric parameters of the DG were optimized within the mathematical modeling by the swarm method. It was shown that the maximum efficiency of radiation input for the selected parameters was 78.7 % (near the telecommunications wavelength of 1550 nm), which is a very good result compared to the DGs, formed directly in the layer TiO_2. Besides, the width of the operating band at the level of -1 dB is 53 nm, which is more than the width C of the band of the DWDM wavelength grid (35 nm). Besides, the optimal thickness of the layer TiO_2 both for the waveguides and for the DGs was 150 nm, which will allow avoiding transition elements in the manufacturing process.

Funding

The study was supported by the Ministry of Science and Higher Education of the Russian Federation, project No. FSWR-2025-0008.

Conflict of interest

The authors state that they have no conflict of interest.

References

[1] B.T. Matthias, J.P. Remeika. Phys. Rev. B, **76**, 1886 (1949). https://doi.org/10.1103/physrev.76.1886.2
[2] R.S. Weis, T.K. Gaylord. Appl. Phys. A, **37**, 191 (1985). https://doi.org/10.1007/BF00614817
[3] E.L. Wooten, G.E. Bethea, R.E. Lampert, D.L. Harvey, D.E. Hagerman, J.J. Wessel, W.S.C. Chang, N.A. Andersen, M.K. Giles, J.N. Jain. IEEE J. Select. Top. Quant. Electron., **6**, 69 (2000). https://doi.org/10.1109/2944.826874
[4] IEEE. The International Roadmap for Devices and Systems^{TM}, 2021 Update. https://irds.ieee.org/images/files/pdf/2021/2021IRDS_MtM.pdf
[5] M. Zhang, C. Wang, R. Cheng, A. Shams-Ansari, M. Lončar. Optica, **4**, 1536 (2017). https://doi.org/10.1364/OPTICA.4.001536
[6] F. Généreux, G. Baldenberger, B. Bourliaguet, R. Vallée. Optics Lett., **32**, 1108 (2007). https://doi.org/10.1364/ol.32.001108
[7] F. Labbé, Ç. Ekici, I. Zhdanov, A.L. Muthali, L.K. Oxenløwe, Y. Ding. Adv. Photon., **7**, 044002 (2025). https://doi.org/10.1117/1.AP.7.4.044002
[8] Y. Hu, D. Zhu, S. Lu, X. Zhu, Y. Song, D. Renaud, D. Assumpcao, R. Cheng, C.J. Xin, M. Yeh, H. Warner, X. Guo, A. Shams-Ansari, D. Barton, N. Sinclair, M. Lončar. Nature Rev. Phys., **7**, 237 (2025). https://doi.org/10.1038/s42254-025-00825-5
[9] G. Chen, N. Li, J.D. Ng, H.L. Lin, Y. Zhou, Y.H. Fu, L.Y.T. Lee, Y. Yu, A.Q. Liu, A.J. Danner. Adv. Photon., **4**, 034003 (2022). https://doi.org/10.1117/1.AP.4.3.034003
[10] A. Boes, B. Corcoran, L. Chang, J. Bowers, A. Mitchell. Laser Photon. Rev., **12**, 1700256 (2018). https://doi.org/10.1002/lpor.201700256
[11] L. He, M. Zhang, A. Shams-Ansari, R. Zhu, C. Wang, M. Lončar. Optics Lett., **44**, 2314 (2019). https://doi.org/10.1364/OL.44.002314
[12] J.L. Han, M.Q. Li, R.B. Wu, J. Yu, L. Gao, Z. Fang, M. Wang, Y. Liang, H. Zhang, Y. Cheng. Opto-Electron. Sci., **4**, 250004 (2025). https://doi.org/10.29026/oes.2025.250004
[13] F. Amanti, G. Andrini, F. Armani, F. Barbato, V. Bellani, V. Bonaiuto, S. Cammarata, M. Campostrini, T.H. Dao, F.D. Matteis, V. Demontis, S. Donati, G. Giuseppe, S.D. Tchernij, A. Fontana, J. Forneris, L. Frontini, R. Gunnella, S. Ladanza, A.E. Kaplan, C. Lacava, V. Liberali, L. Martini, F. Marzioni, L. Morescalchi, E. Pedreschi, P. Piergentili, D. Prete, V. Rigato, C. Roncolato, F. Rossella, M. Salvato, F. Sargeni, J. Shojaii, F. Spinella, A. Stabile, A. Toncelli, V. Vitali. Photonics, **11**, 494 (2024). https://doi.org/10.3390/photonics11060494
[14] S.S.P. Kumar, N.N. Klimov, P.S. Kuo. AIP Advances, **14**, 065317 (2024). https://doi.org/10.1063/6.0003522
[15] M.S. Nisar, X. Zhao, A. Pan, S. Yuan, J. Xia. IEEE Photon. J., **9**, 6600208 (2017). https://doi.org/10.1109/JPHOT.2016.2630314
[16] Z. Ruan, J. Hu, Y. Xue, J. Liu, B. Chen, J. Wang, K. Chen, P. Chen, L. Liu. Opt. Express, **28**, 35615 (2020). https://doi.org/10.1364/OE.411284
[17] S.K. Selvaraja, D. Vermeulen, M. Schaekers, E. Sleeckx, W. Bogaerts, G. Roelkens, P. Dumon, D. Van Thourhout, R. Baets. Proc. Conf. on Lasers and Electro-Optics (CLEO 2009) (Baltimore, MD, USA, 2009) paper CTuC6. https://doi.org/10.1364/CLEO.2009.CTuC6
[18] M. Emsley, O. Dosunmu, M.S. Ünlü. IEEE J. Select. Top. Quant. Electron., **8**, 948 (2002). https://doi.org/10.1109/JSTQE.2002.801692
[19] F. Van Laere, G. Roelkens, M. Ayre, J. Schrauwen, D. Taillaert, D. Van Thourhout, T.F. Krauss, R. Baets. J. Lightwave Technol., **25**, 151 (2007). https://doi.org/10.1109/JLT.2006.888164
[20] Z. Chen, R. Peng, Y. Wang, H. Zhu, H. Hu. Optical Mater. Express, **7**, 4010 (2017). https://doi.org/10.1364/OME.7.004010
[21] Z. Chen, Y. Wang, H. Zhang, H. Hu. Optical Mater. Express, **8**, 1253 (2018). https://doi.org/10.1364/OME.8.001253
[22] X. Han, Y. Jiang, A. Frigg, H. Xiao, P. Zhang, A. Boes, T. Nguyen, J. Yang, G. Ren, Y. Su, Y. Tian. APL Photonics, **6**, 086108 (2021). https://doi.org/10.1063/5.0055213
[23] J. Lee, M.S. Kwon. Optics Lett., **50**, 2133 (2025). https://doi.org/10.1364/OL.555001
[24] L. Li, Yi. Zou, H. Lin, X. Sun, N.-N. Feng, S. Danto, K. Richardson, T. Gu, M. Haney. J. Lightwave Technol., **31**, 4080 (2013). https://doi.org/10.1109/JLT.2013.2285382
[25] H. Huang, K. Liu, B. Qi, V.J. Sorger. J. Lightwave Technol., **34**, 3811 (2016).
[26] Sh. Li, L. Cai, Y. Wang, Y. Jiang, H. Hu. Opt. Express, **23**, 24212 (2015). https://doi.org/10.1364/OE.23.024212
[27] M.S. Nisar, X. Zhao, A. Pan, S. Yuan, J.S. Xia. IEEE Photon. J., **9** (6), 600208 (2017). https://doi.org/10.1109/JPHOT.2016.2630314
[28] F. Yang, H. Fang, H. Han, B. Xiang. Crystals, **12**, 70 (2022). https://doi.org/10.3390/cryst12010070

[29] B. Chen, Z. Ruan, K. Chen, L. Liu. Optics Lett., **48**, 1434 (2023). https://doi.org/10.1364/OL.481277
[30] X. Zhou, Y. Xue, F. Ye, Z. Feng, Y. Li, X. Sun, K.M. Lau, H.K. Tsang. Optics Lett., **48**, 3267 (2023). https://doi.org/10.1364/OL.489753
[31] R. Marchetti, C. Lacava, L. Carroll, K. Gradkowski, P. Minzioni. Photonics Res., **7**, 201 (2019). https://doi.org/10.1364/PRJ.7.000201

Translated by D.Safin